American Mineralogist, Volume 80, pages 247–252, 1995

Sequences of charged sheets in rectorite

HANS J. JAKOBSEN, NIELS C. NIELSEN
Department of Chemistry, University of Aarhus, DK-8000 Aarhus C, Denmark
HOLGER LINDGREEN
Clay Mineralogical Laboratory, Geological Survey of Denmark, DK-2400 Copenhagen NV, Denmark

ABSTRACT

Two rectorite samples, a Na- and Ca-rich rectorite (sample 1) from Beatrix Mine, South Africa, and a Na-rich rectorite (sample 2) from Garland County, Arkansas, have been investigated quantitatively by solid-state ^{23}Na, ^{27}Al, and ^{29}Si magic-angle spinning (MAS) NMR spectroscopy, total chemical dissolution, cation exchange, and X-ray diffraction (XRD). Comparison of modeled and experimental diffractograms shows that both rectorite samples have a mica to smectite ratio of 1:1 and an ideal ordering in units of one mica plus one smectite layer. The average thicknesses of the coherent scattering domains are ten and eight 2:1 layers for samples 1 and 2, respectively. Quantification of the ^{23}Na, ^{27}Al, and ^{29}Si MAS NMR spectra has allowed determination of the compositions for the octahedral sheets and for the mica (paragonite and margarite) and smectite tetrahedral sheets and determination of the distribution of interlayer Na^+ ions between paragonite and margarite interlayers. Each 2:1 layer has an octahedral sheet of weak positive charge sandwiched between two tetrahedral sheets of weak and strong negative charge. The top and bottom tetrahedral sheets of the coherent scattering domains have strong negative charges and very high cation-exchange capacities for sample 1 and low negative charges for sample 2. Sample 1 is a three-component mixed layer (margarite, paragonite, and smectite), and sample 2 a two-component mixed layer (paragonite and smectite).

INTRODUCTION

Recent advances in the methodology of solid state magic-angle spinning (MAS) NMR spectroscopy have proved of special importance to the structural studies of minerals. In particular, in studies of the tetrahedral and octahedral sheets of 2:1 layer phyllosilicates, high-resolution ^{27}Al and ^{29}Si MAS NMR have found widespread usage. In the present work we show that detailed and hitherto unknown information on the compositions, charges, and sequences of the tetrahedral and octahedral sheets, along with the interlayer fixed cations, can be determined for rectorite employing state of the art quantitative ^{23}Na, ^{27}Al, and ^{29}Si MAS NMR combined with XRD and elemental analysis. Two rectorite samples have been investigated, and these show significant differences in compositions, charges, and interlayer cations for the tetrahedral sheets.

Rectorite was initially studied by XRD and elemental analysis in the 1950s. Its structure was thereby determined to be contiguous pairs of pyrophyllite and pairs of mica layers, linked by fixed K^+ and Ca^{2+} ions for the rectorite from Garland County, Arkansas (Bradley, 1950), and from Allevard, France (Brindley, 1956), respectively. Employing infrared spectroscopy and transmission electron microscopy in addition to these methods, Brown and Weir (1965) found that these rectorite samples, plus one from Dagestan and one from Baluchistan, consist of pairs of 2:1 layers and that alternate interlayers are mica-like and smectite-like. Kodama (1966) investigated the Baluchistan rectorite using XRD, elemental analysis, thermal analysis, and infrared spectroscopy and concluded that the structure is a regularly alternating sequence of paragonite-like layers and expandable layers having montmorillonitic and beidellitic compositions. Using the same methods, Gradusov et al. (1968) concluded that the Dagestan rectorite consists of mica-like and montmorillonite-like packets. However, the fundamental particle model of Nadeau et al. (1984) sustained the idea that rectorite consists of mica (or illite) particles 20 Å thick with swelling interparticle spacings. Employing ^{29}Si MAS NMR, Barron et al. (1985a, 1985b) observed that the mica and smectite $^{[4]}Si$ sites in rectorite can be distinguished, and they concluded that the rectorite from North Little Rock, Arkansas, has equal numbers of mica and smectite tetrahedral sheets. Furthermore, ^{29}Si spin-lattice relaxation time measurements, performed by these authors on a Mn^{2+}-exchanged (paramagnetic cation) sample, showed that for this rectorite the interlayers have either two adjacent smectite or two adjacent paragonite tetrahedral sheets. Using the spectral data of Barron et al. (1985a, 1985b), Altaner et al. (1988) calculated that rectorite consists of alternating smectite and mica layers in MacEwan crystallites.

0003–004X/95/0304–0247$02.00

TABLE 1. Compositions of Na- and Ca-rich rectorite (sample 1, Beatrix Mine) and Na-rich rectorite (sample 2, Garland County) per $O_{10}(OH)_2$ formula unit

Rectorite sample	Component	Two tetrahedral sheets: Amount (%)	Two tetrahedral sheets: Composition	One octahedral sheet	Fixed and exchangeable cations for two tetrahedral sheets
	margarite	24	$Al_{2.00}Si_{2.00}$		$(Na_{0.20}Ca_{0.80})_{mar}$
	margarite*	6	$Al_{2.00}Si_{2.00}$		$X_{1.80}$**
	paragonite	16	$Al_{1.32}Si_{2.68}$		$(K_{0.10}Na_{0.78}Ca_{0.12})_{par}$
1	paragonite*	4	$Al_{1.32}Si_{2.68}$	$Mg_{0.02}Fe_{0.01}Al_{2.01}$	$X_{1.12}$
	mica (mean)	50	$Al_{1.73}Si_{2.27}$		$X_{0.31}(K_{0.03}Na_{0.25}Ca_{0.04})_{par}(Na_{0.10}Ca_{0.38})_{mar}$
	smectite	50	$Al_{0.13}Si_{3.87}$		$X_{0.13}$
	total composition		$Al_{0.93}Si_{3.07}$		$X_{0.22}(K_{0.015}Na_{0.125}Ca_{0.02})_{par}(Na_{0.05}Ca_{0.19})_{mar}$
	paragonite	50	$Al_{1.24}Si_{2.76}$		$(Na_{0.96}Ca_{0.02})_{par}$
2	smectite	50	$Al_{0.24}Si_{3.76}$	$Mg_{0.01}Fe_{0.03}Al_{2.00}$	$X_{0.24}$
	total composition		$Al_{0.74}Si_{3.26}$		$X_{0.12}(Na_{0.49}Ca_{0.01})_{par}$

Note: compositions determined from ^{29}Si, ^{27}Al, and ^{23}Na MAS NMR combined with Ca, K, Mg, and Fe data from elemental analysis. The total composition for sample 1 may, for example, be represented by a mixture of the particles A (60%) and B (40%) shown in Fig. 3. An impurity of dickite, 12 mol% calculated from ^{27}Al and ^{29}Si MAS NMR and ≈15 mol% (≈10 wt%) from elemental analysis, was observed for sample 2 in accordance with earlier reports for rectorite samples from this location (Brown and Weir, 1965).

* Top and bottom tetrahedral mica sheets.

** X is a monovalent cation equivalent of the exchangeable cations for the smectite layers and top and bottom tetrahedral sheets.

SAMPLES AND EXPERIMENTAL TECHNIQUES

Samples of a Na- and Ca-rich rectorite (sample 1) from Beatrix Mine, South Africa, and a Na-rich rectorite (CMS RAr-1) (sample 2) from Garland County, Arkansas, U.S.A., were investigated. A small impurity of calcite (≈6 wt%; detected by XRD) in sample 1 was removed prior to the NMR and elemental analysis. For sample 2, XRD detected a minor impurity of dickite (8–10 wt% calculated from chemical analysis and NMR) that could not be removed but was compensated for in the calculations of the quantitative results. Natural samples and Na^+- and Mg^{2+}-exchanged samples were investigated by NMR and elemental analysis.

XRD experimental patterns were obtained for oriented samples prepared by evaporating and drying a suspension of Mg^{2+}-exchanged clay on a glass slide, followed by ethylene glycol intercalation achieved by exposing this specimen to ethylene glycol at 60 °C for 3 d. A Philips diffractometer and Co$K\alpha$ radiation were used with a PW1050 goniometer having fixed divergence and scatter slits, ¼° from 3–18° 2θ and 1° from 18–36° 2θ. Monochromatization was obtained by use of a β filter and pulse-height selection. The calculated patterns were obtained with the Newmod computer program of R. C. Reynolds (Dartmouth College). The calculations assumed no Fe but allowed for Na and Ca in the mica interlayers as indicated in Table 1, together with the defect broadening of Ergun (1970).

The ^{23}Na, ^{27}Al, and ^{29}Si MAS NMR spectra were recorded on Varian XL-300 (7.1-T) and UNITY-400 (9.4-T) spectrometers equipped with home-built high-speed MAS probes (Jakobsen et al., 1988) for ceramic rotors with outside diameters of 7 and 5 mm, which allow spinning speeds up to 11 and 16 kHz, respectively, to be employed. To obtain quantitatively reliable spectra, sufficiently long relaxation delays (estimated from T_1 measurements) were used for all three nuclei. The ^{23}Na and ^{27}Al MAS NMR spectra were acquired using a flip angle of $\pi/12$ and an RF field strength $\gamma B_1/2\pi$ = 60 kHz to ensure accurate relative intensities (e.g., for the $^{[4]}Al$ and $^{[6]}Al$ resonances). To avoid overlap of spinning sidebands with the central transitions and to observe the complete spinning sideband pattern of the satellite transitions (Jakobsen et al., 1989), the ^{27}Al MAS experiments were performed with spinning speeds up to 15 kHz using spectral widths of 2 MHz. The ^{23}Na, ^{27}Al, and ^{29}Si chemical shifts are reported relative to external samples of 1.0 M NaCl, 1.0 M $AlCl_3$, and TMS, respectively. Relative intensities were evaluated by deconvolution (iterative fitting) of the experimental spectra on the Sun computer of the UNITY-400 spectrometer.

RESULTS AND DISCUSSION

Rectorite ordering

XRD shows the smectite + mica superstructure of rectorite with equal numbers of smectite and mica periods for samples 1 (Fig. 1) and 2. For d_{001}–d_{009} in the glycolated specimens, the coefficient of variation for the d values is 0.41 and 0.12 for samples 1 and 2, respectively, i.e., well below the maximum of 0.75 for adequate regular alternation (Bailey et al., 1982). According to the calculated patterns, the rectorite samples consist of 50% mica and 50% smectite layers with R1 ordering. Modeled d_{001} values for the smectite and mica layers are 17.13 and 9.45 Å, respectively, for both glycolated rectorite samples, whereas the smectite spacings for the air-dried specimens are 14.9 and 14.6 Å for samples 1 and 2, respectively. The mica layer thickness of 9.45 Å is slightly lower than for margarite (9.55 Å) or for paragonite (9.65 Å) but larger than for pyrophyllite (9.20 Å) (Bailey, 1980). The average thickness of the coherent scattering domains is ten and eight 2:1 layers for samples 1 and 2, respectively. From XRD, mica and smectite are distinguished mainly by the d_{001} values of the 2:1 layers. Differences in scattering from interlayer cations are minor, and the substitution of Al for Si in the tetrahedral mica sheets has neg-

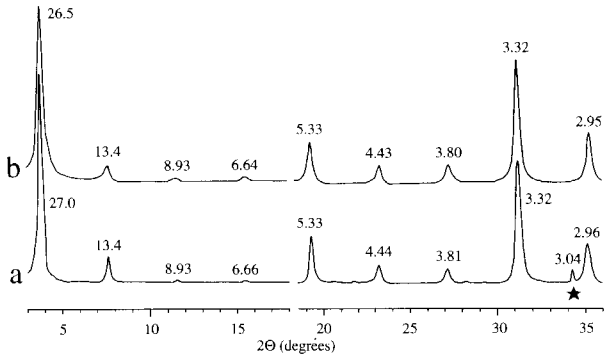

Fig. 1. Experimental (a) and calculated (b) XRD patterns for the rectorite sample 1; peaks are labeled with *d* values in ångströms. The peak marked with a star at 3.04 Å is due to calcite.

ligible effects on XRD. Thus, XRD cannot determine whether the top and bottom tetrahedral sheets in the coherent scattering domains are smectitic or micaceous.

Tetrahedral sheets

The compositions of the tetrahedral mica and smectite sheets and the significant structural differences between samples 1 and 2 are most easily determined from their high-resolution ^{29}Si MAS NMR spectra (Fig. 2). The spectrum of sample 2 (Fig. 2b) is rather similar to that reported earlier for the rectorite from North Little Rock, Arkansas, U.S.A. (Barron et al., 1985a, 1985b), whereas the spectrum of sample 1 (Fig. 2a) exhibits a quite different distribution of peak intensities. Thus, in the following discussion mainly the data of the experimental results for sample 1 are emphasized; the differences in the structures for samples 1 and 2 are apparent from Table 1 and Figure 3. The ^{29}Si spectra show not only separate ^{29}Si resonances for the smectite and mica sheets but also resolution of the individual resonances according to the Si(*n*Al) substitution pattern within these sheets; the nomenclature

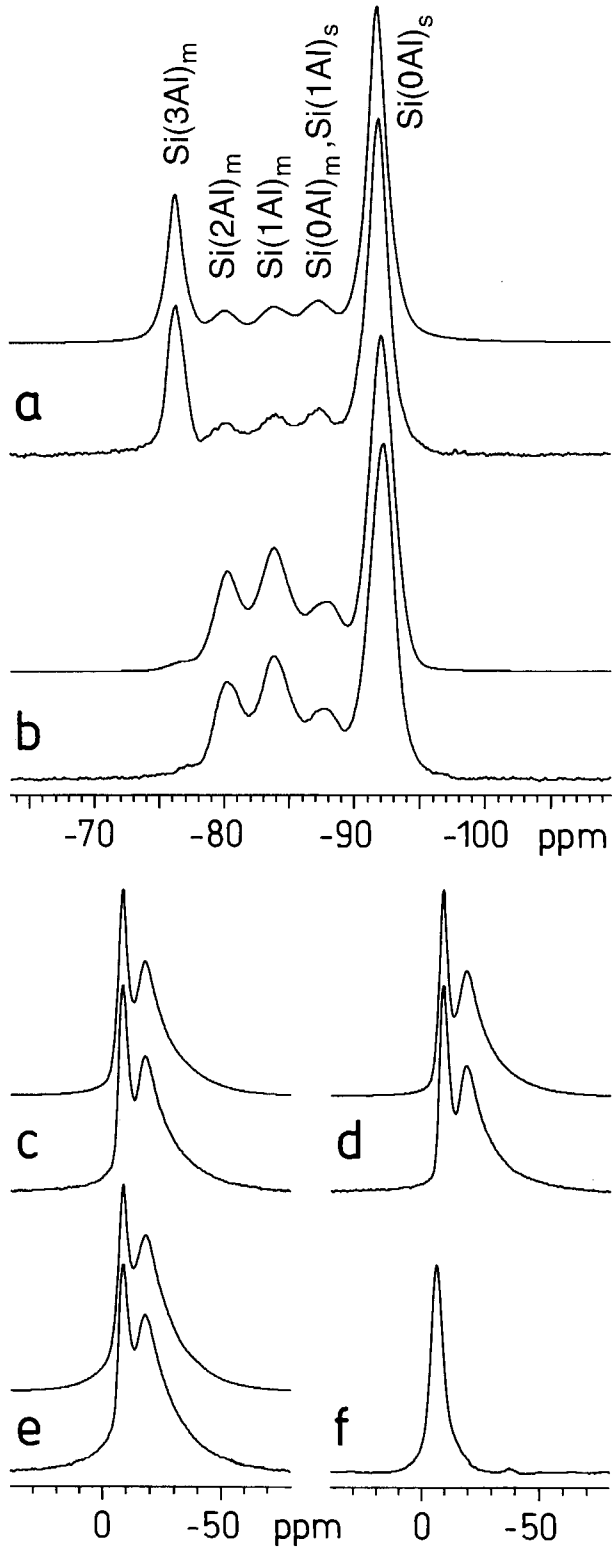

→

Fig. 2. Fully relaxed ^{29}Si MAS NMR spectra for the rectorite samples 1 (a) and 2 (b). The upper traces in a and b represent the final results for the deconvolutions of the experimental spectra; the corresponding relative intensities for sample 1 are given in the text. The symbols Si(*n*Al)$_m$ and Si(*n*Al)$_s$ next to the peaks indicate the assignment of the ^{29}Si resonances for the mica (margarite and paragonite for sample 1 and paragonite for sample 2) and smectite layers, respectively. The relative intensities of the overlapping resonances for Si(0Al)$_m$ and Si(1Al)$_s$ were evaluated from T_1 ^{29}Si spin-lattice relaxation time experiments, employing the difference in T_1 (^{29}Si) values for mica and smectite and the method outlined by Barron et al. (1985b). The ^{23}Na MAS NMR spectra for sample 1: (c) natural sample, (d) Mg^{2+}-exchanged, and (e) Na^+-exchanged. (f) A ^{23}Na MAS NMR spectrum for a sample of margarite. The upper traces in c–e show the deconvolutions for the three experimental spectra of sample 1 for determination of the relative intensities of the two peaks (see text).

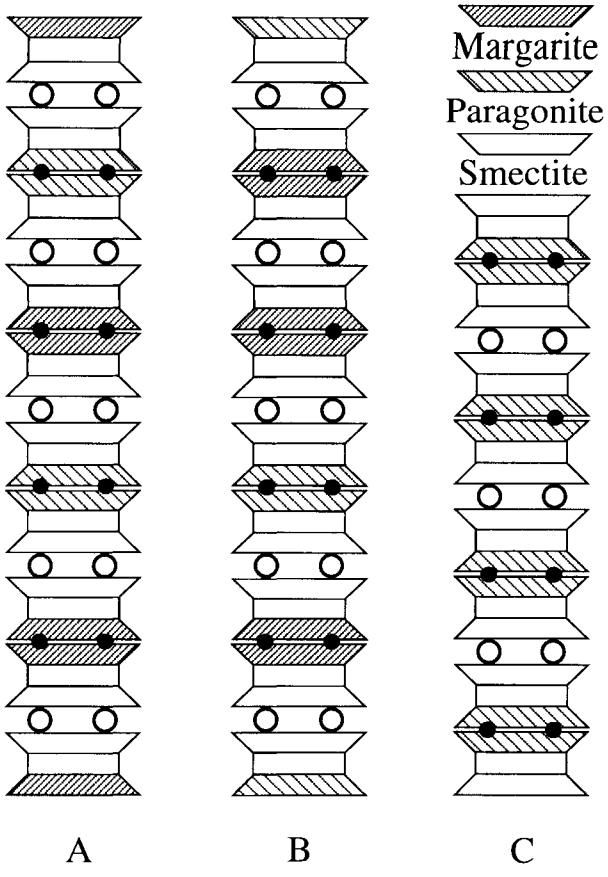

Fig. 3. MacEwan particles representing the structures determined for the two rectorite clay minerals in this study. Sample 1 may be represented, for example, by a mixture of particles A (60%) and B (40%) and sample 2 by particle C. For each particle the 2:1 layers with tetrahedral (margarite, paragonite, or smectite), octahedral, and tetrahedral sheets are shown enclosed by interlayer cations (open and solid circles). Open circles represent exchangeable, hydrated cations, and solid circles are fixed, dehydrated cations.

Si(nAl) designates a Si atom bonded (by O atoms) to n[4]Al atoms in a tetrahedral sheet (n = 0–3). The relative Si(nAl) intensities determined for sample 1 (Fig. 2) within and between the mica [16(0Al):75(1Al):61(2Al):212(3Al)] and smectite sites [571(0Al):65(1Al):0(2Al):0(3Al)] reveal a high degree of [4]Al substitution and an unusual substitution pattern for the mica tetrahedral sheets in this rectorite. This substitution pattern for the mica sheets in sample 1 deviates strongly from the approximate binomial Si(nAl) intensity distribution generally observed for substitution of Al for Si in micas (e.g., for the mica sheets in sample 2). Because of the large intensity observed for the mica Si(3Al) resonance in sample 1, we propose the presence of two different mica sheets in sample 1, a proposal borne out by the ^{23}Na MAS experiments described below, but not apparent in the XRD d values. One sheet is margarite [$\delta = -76.3$ ppm (Kinsey et al., 1985), Si(3Al)], with a tetrahedral layer composition of $Si_{2.0}Al_{2.0}$ per $O_{10}(OH)_2$. The other mica sheet is paragonite, with an approximate binomial Si(nAl) intensity distribution [16(0Al):75(1Al):61(2Al):19(3Al)] corresponding to a layer composition of $Si_{2.68}Al_{1.32}$. The layer compositions were determined from the Si-Al ratios calculated from the relative Si(nAl) intensities, I_n, using the equation (Engelhardt and Michel, 1987)

$$\frac{\text{Si}}{\text{Al}} = 3 \sum_{n=0}^{3} I_n \Big/ \sum_{n=0}^{3} nI_n.$$

Following a moment analysis of the ^{29}Si NMR spectra of the tetrahedral sheets similar to the procedure outlined by Vega (1983) for framework Si, we note that Loewenstein's avoidance principal (no Al-O-Al bonds) applies for both rectorite samples. Employing the average thickness of ten 2:1 layers for the sample 1 particles from XRD, we find that the ^{29}Si NMR intensities correspond to exactly 50% smectite layers ($Si_{3.87}Al_{0.13}$), along with 30% margarite and 20% paragonite tetrahedral sheets.

Exchangeable and fixed cations

The interlayer cations fixed between the mica layers of sample 1 consist of approximately equal numbers of Na^+ and Ca^{2+}, according to the elemental analysis. However, quantitative ^{23}Na MAS NMR spectra of natural, Na^+-exchanged, and Mg^{2+}-exchanged samples of 1 (Fig. 2c–2e) and 2 (not shown) allow determination of the distribution of Na^+, not only between the cation-fixed (in interlayer mica sheets) and cation-exchangeable positions (in smectite sheets and at the top and bottom tetrahedral sheets of the particle), but also, as shown below, between the fixed interlayer positions of margarite and paragonite for sample 1. The ^{23}Na NMR spectra of the three samples of 1 (Fig. 2c–2e) all exhibit a rather narrow resonance ($\delta = -8.3$ ppm) of constant intensity, which partially overlaps with a broader peak ($\delta \approx -18$ ppm) of varying intensity. The chemical shift of the narrow resonance is similar to the ^{23}Na shift observed by us for two samples of margarite (Fig. 2f, $\delta = -5.0$ ppm) and is assigned to Na^+ fixed between margarite tetrahedral sheets in which Ca^{2+} is the predominant fixed interlayer cation. The intensity ratios between the narrow resonance ($\delta = -8.3$ ppm) and the broad resonance for the three samples are 0.32 (Fig. 2c), 0.37 (Fig. 2d), and 0.17 (Fig. 2e). The broader peak observed for the three samples (1, Fig. 2c–2e) has a similar appearance, intensity variation, and resonance position as those observed for the ^{23}Na resonance of the three samples of 2 for which only a single broad resonance is observed at $\delta \approx -18$ ppm. Thus, this resonance is assigned to overlap between Na^+ fixed between paragonite tetrahedral sheets and exchangeable Na^+. Our ^{23}Na NMR results for sample 1 therefore demonstrate that interlayers with fixed cations have either two adjacent margarite or two adjacent paragonite tetrahedral sheets, but not one of each. A similar pattern of sheet pairing has previously been observed for the North Little

Rock rectorite (Barron et al., 1985b), where interlayers have either two smectite or two paragonite tetrahedral sheets adjacent.

Octahedral sheets

Values for d_{060} of 1.484 and 1.485 Å for samples 1 and 2, respectively, demonstrate that the octahedral sheets of both rectorite samples are dioctahedral. The octahedral sites are occupied by Al and trace amounts of Mg and Fe, according to the elemental analysis (Table 1). The ^{27}Al MAS NMR spectra of samples 1 and 2 show that the octahedral and tetrahedral Al have approximately equal quadrupole coupling constants C_Q; actually, the two sites are characterized by a distribution of C_Q values ($C_Q \approx 2$–3 MHz), as judged from the appearance of the spinning sideband intensities for the satellite transitions (Jakobsen et al., 1989). Therefore, reliable quantitative ^{27}Al MAS NMR experiments are easily performed at high-speed spinning, and for sample 1 we obtain the ratio of $^{[4]}$Al to $^{[6]}$Al = 0.47. This ratio, combined with the ^{29}Si NMR results for the compositions ($Si_{4-x}Al_x$) and percentages of the three different tetrahedral sheets in sample 1, shows that the octahedral sheets have ~2.0 Al per $O_{10}(OH)_2$. The negative charges of the margarite and paragonite tetrahedral sheets are, however, both larger (−0.10 per sheet) than the compensating positive charges of their fixed interlayer cations. This surplus negative charge must therefore be compensated for by an octahedral sheet of composition ($Mg^{2+}_{0.02}$ $Fe^{3+}_{0.01}$ $Al^{3+}_{2.01}$), which contributes a charge of +0.10 and is consistent with the elemental analysis. A positive octahedral charge in rectorite has previously been calculated by Brown and Weir (1965) and Kodama (1966) [+0.23 and +0.16 per $O_{10}(OH)_2$, respectively].

Structures of the domain top and bottom tetrahedral sheets and MacEwan particles

The high cation-exchange capacity for sample 1, determined from ^{23}Na MAS NMR and by elemental analysis of the three samples in Figure 2c–2e, cannot be attributed solely to the low negative charge of the smectite layers as calculated from the ^{29}Si NMR spectrum (Fig. 1). Within the coherent scattering domains ten 2:1 layers thick, additional mica tetrahedral sheets adjacent to swelling interlayers and contributing to the exchange capacity are unlikely for rectorites. This follows from the pattern of sheet pairing demonstrated above by the ^{23}Na NMR results and also demonstrated by the ^{29}Si spin-lattice relaxation times determined here and previously (Barron et al., 1985b) for the North Little Rock rectorite employing a paramagnetic reporter ion, Mn^{2+}. This pattern of sheet pairing conforms with the high degree of regularity of swelling, as demonstrated by the low coefficient of variation for d_{001} of 0.41. An interlayer spacing between one smectite and one mica tetrahedral sheet (the mica sheet being paragonite or margarite, with a negative charge of −0.66 and −1.0, respectively) is unlikely to swell in the same manner as does an interlayer spacing between two adjacent smectite tetrahedral sheets. For example, vermiculite, which has a tetrahedral sheet charge of similar magnitude (−0.6 to −0.9) adjacent to the interlayers, shows limited swelling. Therefore, an additional exchange capacity must arise from margarite or paragonite tetrahedral sheets at the top and bottom of the crystallite particles (Fig. 3). In fact, for sample 1 the number of exchangeable cations corresponds to the total negative charge of the smectite and top and bottom mica tetrahedral sheets (Fig. 3 and Table 1). However, for sample 2 the exchange capacity is due to smectite interlayers and top and bottom smectite tetrahedral sheets (Table 1, Fig. 3). The rectorite structure with fundamental mica particles 20 Å thick (Nadeau et al., 1984) is not valid for the two natural (hydrothermal) rectorite samples. According to our results, the structure of the two rectorite samples is accurately described as being coherently scattering MacEwan particles. Although our data from NMR and XRD represent averages for a distribution of MacEwan crystallite sizes (e.g., with a mean of coherent scattering domains ten 2:1 layers thick for sample 1), we find that for sample 1 an average of, for example, two MacEwan particles (60% A and 40% B, Fig. 3) is consistent with the charges and compositions determined, and for sample 2 one MacEwan particle (C in Fig. 3) is consistent.

Our results demonstrate that the alternation of high- and low-charge tetrahedral sheets in the 2:1 layers of rectorite results in high-charge top and bottom tetrahedral sheets in one sample and low-charge in the other. Finally, the nature of the tetrahedral sheets at the top and bottom of the particles has important implications for the exchange and catalytic properties of these minerals.

Acknowledgments

We thank V.A. Drits, B.A. Sakharov, and S. Altaner for helpful discussions and two reviewers for fruitful comments. The use of the facilities at the University of Aarhus NMR Laboratory, sponsored by Teknologistyrelsen, the Danish Research Councils (SNF and STVF), Carlsbergfondet, and Direktør Ib Henriksens Fond, is acknowledged. We thank Aarhus University Research Foundation for equipment grants.

References cited

Altaner, S.P., Weiss, C.A., and Kirkpatrick, R.J. (1988) Evidence from ^{29}Si NMR for the structure of mixed-layer illite/smectite clay minerals. Nature, 351, 699–702.

Bailey, S.W. (1980) Structures of layer silicates. In G.W. Brindley and G. Brown, Eds., Crystal structures of clay minerals and their X-ray identification, p. 1–123. Mineralogical Society, London.

Bailey, S.W., Brindley, G.W., Kodama, H., and Martin, R.T. (1982) Report of the clay minerals society nomenclature committee for 1980–1981: Nomenclature for regular interstratifications. Clays and Clay Minerals, 30, 76–78.

Barron, P.F., Slade, P., and Frost, R.L. (1985a) Solid-state silicon-29 spin-lattice relaxation in several 2:1 phyllosilicate minerals. Journal of Physical Chemistry, 89, 3305–3310.

——— (1985b) Ordering of aluminum in tetrahedral sites in mixed-layer 2:1 phyllosilicates by solid-state high-resolution NMR. Journal of Physical Chemistry, 89, 3880–3885.

Bradley, W.F. (1950) The alternating layer sequence of rectorite. American Mineralogist, 35, 590–595.

Brindley, G.W. (1956) Allevardite, a swelling double-layer mica mineral. American Mineralogist, 41, 91–103.

Brown, G., and Weir, A.H. (1965) The identity of rectorite and allevar-

dite. In I.T. Rosenqvist and P. Graff-Petersen, Eds., Proceedings of the International Clay Conference Stockholm, 1, p. 27–35. Pergamon, Oxford, U.K.

Engelhardt, G., and Michel, D. (1987) High resolution solid state NMR of silicates and zeolites, 150 p. Wiley, Chichester, U.K.

Ergun, S. (1970) X-ray scattering by very defective lattices. Physics Review B, 131, 3371–3380.

Gradusov, B.P., Chizhikova, N.P., and Travnikova, L.S. (1968) The nature of interlayer spaces in rectorite from Dagestan. Doklady Akademii Nauk SSSR Earth Science Section, 180, 130–132.

Jakobsen, H.J., Daugaard, P., and Langer, V. (1988) CP/MAS NMR at high speeds and high fields. Journal of Magnetic Resonance, 76, 162–168.

Jakobsen, H.J., Skibsted, J., Bildsøe, H., and Nielsen, N.C. (1989) Magic-angle spinning NMR spectra of satellite transitions for quadrupolar nuclei in solids. Journal of Magnetic Resonance, 80, 173–180.

Kinsey, R.A., Kirkpatrick, R.J., Hower, J., Smith, K.A., and Oldfield, E. (1985) High resolution aluminum-27 and silicon-29 nuclear magnetic resonance spectroscopic study of layer silicates, including clay minerals. American Mineralogist, 70, 537–548.

Kodama, H. (1966) The nature of the component layers in rectorite. American Mineralogist, 51, 1035–1055.

Nadeau, P.H., Wilson, M.J., McHardy, W.J., and Tait, J.M. (1984) Interparticle diffraction: A new concept for interstratified clays. Clay Minerals, 19, 757–769.

Vega, A.J. (1983) A statistical approach to the interpretation of silicon-29 NMR of zeolites. In G.D. Stucky and F.G. Dwyer, Eds., Intrazeolite chemistry, p. 217–230. American Chemical Society Symposium Series, 218.

Manuscript received August 22, 1994
Manuscript accepted November 21, 1994